Collinear scattering and long-lived excitations in two-dimensional electron fluids

Serhii Kryhin⬤ and Leonid Levitov⬤

Department of Physics, Massachusetts Institute of Technology, Cambridge, Massachusetts 02139, USA

For a long time, it has been thought that two-dimensional (2D) Fermi gases could support long-lived excitations, owing to the collinear quasiparticle scattering controlled by phase-space constraints at a 2D Fermi surface. We present a direct calculation that reveals such excitations. The excitation lifetimes are found to exceed the fundamental bound set by the Landau Fermi-liquid theory by a factor as large as $(T_F/T)^\alpha$ with $\alpha \approx 2$. These excitations represent Fermi-surface modulations of an odd parity, one per each odd angular momentum. To explain this surprising behavior, we employ a connection between the linearized quantum kinetic equation and the dynamics of a fictitious quantum particle moving in a 1D reflectionless sech^2 potential. In this framework, we identify the long-lived excitations in Fermi gases as zero modes that arise from supersymmetry.

A microscopic theory of carrier collisions in two-dimensional (2D) electron systems is essential for the field of electron hydrodynamics, an area that has made significant progress in recent years [1–19]. The theory of Fermi liquids that links carrier collision rates and quasiparticle lifetimes is generally considered to be comprehensive and complete. However, recent research has challenged the widely held belief that the theory is entirely free of gaps and inconsistencies [20–24]. Specifically, this literature indicates that Landau's T^2 scaling law, which describes quasiparticle decay in three-dimensional (3D) Fermi liquids at low temperatures, may not hold true for 2D metals. This happens because 2D fermions display two-body scattering of a unique collinear character, arising due to kinematic phase-space constraints at the Fermi surface. These findings have interesting implications for our understanding of Fermi liquids, as they suggest that the behavior of quasiparticles in 2D materials may differ significantly from that in 3D materials. The quenching of Landau's T^2 damping for certain excitations points to new ways for extending coherence in electron systems. The aim of this Letter is to validate these predictions through a direct calculation.

The collinear behavior in 2D raises an interesting comparison with one-dimensional (1D) systems, where collinear scattering causes quasiparticles to have a short lifespan. Interactions in 1D systems destroy the Fermi-liquid state, leading to a state known as the Tomonaga-Luttinger state [25,26]. The collinear processes in 2D metals take on a role which is the complete opposite of that in 1D liquids. These processes give a giant boost to quasiparticle lifetimes and can be said to produce a "super Fermi liquid" that harbors a unique family of excitations with exceptionally long lifetimes, exceeding by orders of magnitude those familiar from Fermi-liquid theory. The unique behavior arising from these processes endows the kinetics of 2D fermions with angular memory and gives rise to peculiar "tomographic" response effects [22–24].

The presence of long-lived degrees of freedom can significantly enhance the response to weak perturbations, leading to the emergence of long-lasting collective memory effects and novel hydrodynamic modes. In this regard, recent work [27] predicts the existence of a distinct family of viscous modes characterized by non-Newtonian viscosity. These modes were not anticipated by earlier studies, highlighting the importance of the long-lived degrees of freedom originating from collinear scattering for 2D electron transport.

The emergence of novel timescales is particularly evident in a system with isotropic band dispersion and a circular Fermi surface. In such a system, various excitations correspond to distinct angular harmonics of Fermi-surface modulations that evolve in space and time as

$$\delta f(\boldsymbol{p}, \boldsymbol{x}, t) \sim \sum_m \alpha_m(\epsilon, \boldsymbol{x}, t) \cos m\theta + \beta_m(\epsilon, \boldsymbol{x}, t) \sin m\theta,$$

where θ is the angle parametrizing the Fermi surface. The microscopic decay rates, illustrated in Fig. 1, govern the dynamics of spatially uniform excitations, $\alpha_m, \beta_m \sim e^{-\gamma_m t}$. As evident in Fig. 1, at low temperatures $T \ll T_F$ the lifetimes of these modes greatly exceed the ones for even m, showing a strong departure from conventional Fermi-liquid scaling. The decay rates in Fig. 1 are obtained by a direct calculation that treats quasiparticle scattering exactly, using a method that does not rely on the small parameter $T/T_F \ll 1$. The odd-m decay rates display scaling $\gamma \sim T^\alpha$ with super-Fermi-liquid exponents $\alpha > 2$. In our analysis we find α values close to 4, i.e., the odd-m rates are strongly suppressed compared to the even-m rates, $\gamma_{\text{odd}}/\gamma_{\text{even}} \sim (T/T_F)^2$.

Is there a simple explanation for why the odd-m harmonics are found to be long lived? These harmonics are essentially the perturbations in the particle momentum distribution associated with angle-resolved current, the quantities odd under $\boldsymbol{p} \to -\boldsymbol{p}$ that can take different values on different patches of the Fermi surface. The significance of these "tomographic" quantities is that they are approximately conserved when two-body collisions have a strongly collinear character. In comparison, for two-body collisions in a classical gas, the p-wave ($m = 1$) harmonic of current is conserved, whereas higher-order harmonics ($m = 3$, 5, etc.) are nonconserved. However, in Fermi gases, as discussed below, the collisions are strongly collinear. This property endows all angular
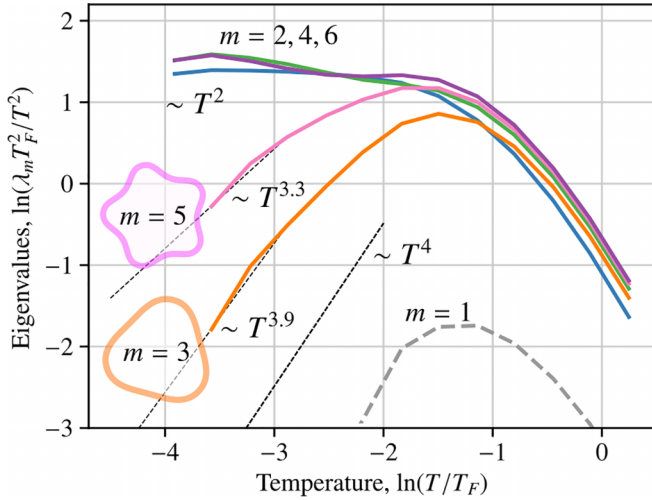
FIG. 1. Decay rates for different angular harmonics of particle distribution, scaled by T^2, vs temperature. Shown are dimensionless eigenvalues λ_m related to the decay rates through $\gamma_m = A p_F^2 \lambda_m$ [see Eq. (4) in Supplemental Material [35]]. A double-log scale is used to facilitate a comparison of disparate timescales. Decay rates for even-m harmonics obey a T^2 scaling at $T \ll T_F$. Decay rates for odd-m harmonics are markedly smaller than those for even m and show "super-Fermi-liquid" scaling strongly deviating from T^2. Odd-m decay rates can be approximated as T^α with $\alpha > 2$. An even/odd asymmetry in the rates and the suppression of decays for odd m is seen already at $T \lesssim 0.16 T_F$.

harmonics of the current, that is, the odd-m harmonics of particle distribution, with exceptionally long lifetimes.

It is worth noting that the absence of Landau's T^2 damping in odd-m modes may seem to contradict the results in the literature on excitation lifetimes in 2D Fermi gases, which predict that quasiparticle lifetimes are diminished by collinear scattering, as revealed by self-energy calculations of Green's functions [28–34]. The predicted decay rates were found to be faster by a logarithmic factor $\log(T_F/T)$ compared to the conventional T^2 rates. Surprisingly, the self-energy approach fails to account for the existence of long-lived odd-m excitations. This is unexpected because it is commonly assumed that there is a single timescale that characterizes decay for all low-energy excitations. However, as shown in Fig. 1, the odd-m and even-m modes have drastically different lifetimes that exhibit different scaling behavior with respect to T. The conventional self-energy approach falls short in effectively addressing this particular situation as it primarily emphasizes the fastest decay pathways, thereby neglecting the presence of long-lived excitations. Surprisingly, despite an extensive and fervent interest in the field of Fermi liquids spanning over 60 years, the long-lived excitations have been overlooked in the existing literature.

We want to emphasize that the collinear processes that generate long-lived excitations are universal and largely independent of the specifics of two-body interactions or particle dispersion characteristics. The existence of long-lived excitations is a robust property that persists for noncircular Fermi surfaces, as long as the surface distortion is not significant. This is due to the presence of inversion symmetry, which

separates Fermi-surface modulations into even- and odd-parity modes. Similar to the self-energy analysis [28–34], the difference in lifetimes between these mode types is identical to that observed in circular Fermi surfaces.

It is worth noting that in certain electron systems, collinear dynamics can accelerate quasiparticle decay by allowing particles, by traveling side by side, to interact more strongly. This is well documented in Dirac bands where collinear dynamics arising from linear band dispersion shortens carrier lifetimes and accelerates dynamics [36–43]. In our problem, an entirely different behavior arises due to collinear scattering and phase-space constraints, the effects that dominate at a 2D Fermi surface but are of little importance for highly excited states in Dirac bands.

The analysis presented below is based on the Fermi-liquid transport equation that accounts for the kinetics of two-body collisions constrained by fermion exclusion,

$$\frac{df_1}{dt} + [f_1, H] = \sum_{21'2'} (w_{1'2' \to 12} - w_{12 \to 1'2'}), \quad (1)$$

where $f(\boldsymbol{p}, \boldsymbol{r}, t)$ is fermion distribution, $[f, H]$ denotes the Poisson bracket $\nabla_{\boldsymbol{r}} f \nabla_{\boldsymbol{p}} \epsilon - \nabla_{\boldsymbol{r}} \epsilon \nabla_{\boldsymbol{p}} f$. The right-hand side is the rate of change of the occupancy of a state $\boldsymbol{p}_1$, given as a sum of the gain and loss contributions resulting from the two-body scattering processes $12 \to 1'2'$ and $1'2' \to 12$. Fermi's golden rule yields

$$w_{1'2' \to 12} = \frac{2\pi}{\hbar} |V_{12,1'2'}|^2 \delta_\epsilon \delta_{\boldsymbol{p}} (1 - f_1)(1 - f_2) f_{1'} f_{2'}, \quad (2)$$

where the delta functions $\delta_\epsilon = \delta(\epsilon_1 + \epsilon_2 - \epsilon_{1'} - \epsilon_{2'})$, $\delta_{\boldsymbol{p}} = \delta^{(2)}(\boldsymbol{p}_1 + \boldsymbol{p}_2 - \boldsymbol{p}_{1'} - \boldsymbol{p}_{2'})$ account for the energy and momentum conservation. The gain and loss contributions are related by the reciprocity symmetry $12 \leftrightarrow 1'2'$. Here, $V_{12,1'2'}$ is the two-body interaction, properly antisymmetrized to account for Fermi statistics. Interaction $V_{12,1'2'}$ depends on momentum transfer k on the $k \sim k_F$ scale; this k dependence is inessential and will be ignored. In what follows we consider a spatially uniform problem setting $[f, H] = 0$. The sum over momenta $2, 1', 2'$ represents a six-dimensional integral over $\boldsymbol{p}_2$, $\boldsymbol{p}_{1'}$, and $\boldsymbol{p}_{2'}$, which is discussed below.

For a weak perturbation away from equilibrium, Eq. (2) linearized by the standard ansatz $f(\boldsymbol{p}) = f_0(\boldsymbol{p}) - \frac{\partial f_0}{\partial \epsilon} \eta(\boldsymbol{p})$, where $f_0(p)$ denotes the equilibrium Fermi distribution, yields a linear integrodifferential equation $f_0(1 - f_0)\frac{d\eta_1}{dt} = I_{ee}[\eta]$ with the operator I_{ee} given by

$$I_{ee}[\eta] = \sum_{21'2'} \frac{2\pi}{\hbar} |V|^2 F_{121'2'} \delta_\epsilon \delta_{\boldsymbol{p}} (\eta_{1'} + \eta_{2'} - \eta_1 - \eta_2). \quad (3)$$

Here, $\sum_{21'2'}$ and $|V|^2$ denote the six-dimensional integral $\int \frac{d^2 p_2 d^2 p_{1'} d^2 p_{2'}}{(2\pi)^6}$ and the interaction matrix element $|V_{12,1'2'}|^2$, whereas the quantity $F_{121'2'}$ is a product of the equilibrium Fermi functions $f_1^0 f_2^0 (1 - f_{1'}^0)(1 - f_{2'}^0)$.

Different excitations are described as eigenfunctions of the collision operator I_{ee}, with the eigenvalues giving decay rates equal to inverse lifetimes. Because of the cylindrical symmetry of the problem, the eigenfunctions are products of angular harmonics on the Fermi surface and functions of the
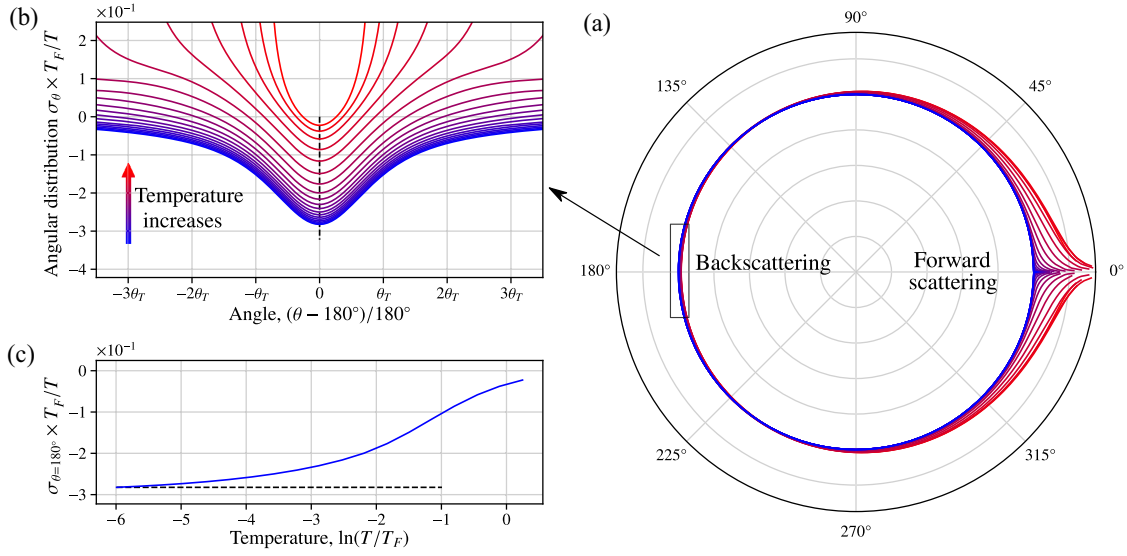
FIG. 2. (a) Angular distribution $\sigma(\theta)$ for two-body quasiparticle scattering at the Fermi surface [Eq. (5)] at different temperatures. Restricted phase space gives rise to collinear scattering, producing sharp peaks in the forward and backward directions, $\theta = 0$ and π. Temperature values used: $T/T_F = 10^{-2} \times [0.25, 0.5, 1, 2, 4, 8, 16, 32, 64, 128]$. (b) The backscattering peak in $\sigma(\theta)$ near $\theta = \pi$ for the same temperatures as in (a). The angle is given in T-dependent units $\theta_T = T/T_F$ to illustrate the linear T dependence of the peak width. The intensity $\sigma(\theta)$ is multiplied by T_F/T to illustrate the linear T dependence of the peak height. This translates into $\sim T^2$ scaling for the peak area. (c) The dependence of peak height vs T confirms asymptotic linear scaling at low T.

radial energy variables $x_i = \beta(\epsilon_i - \mu)$,

$$\eta(\boldsymbol{p}, t) = \sum_m e^{-\gamma_m t} e^{im\theta} \chi_m(x), \qquad (4)$$

where γ_m and $\chi_m(x)$ are solutions of the spectral problem $-\gamma_m f_0(1 - f_0)\chi_m(x) = I_{\mathrm{ee}}[\chi_m(x)]$.

Before we proceed with diagonalizing the operator I_{ee} we note that one more reason for why the long-lived modes have been missed in the literature undoubtedly lies in the difficulty of a direct calculation. This problem proves to be quite demanding for several reasons. First, the eigenstates of I_{ee} are localized in a peculiar phase-space region, an annulus at the Fermi surface of width proportional to T owing to the fermion exclusion effects (see Sec. A in Supplemental Material [35]). Sampling this "active part" of p space requires a mesh which is adjusted with temperature. Second, capturing the kinematic constraints that lead to collinear collision effects, requires "high-finesse" sampling of the near-collinear momenta as compared to the generic momenta in the annulus (see Sec. B in Supplemental Material [35]). The situation is made even more complex by the fact that the angular width of the active collinear region also varies with temperature, decreasing as T. To tackle this problem, we make use of the cylindrical symmetry of our system and link the decay rates for different modes to the angular distribution for scattering induced by a test particle injected in the system. Computing the angular distribution as described below, we Fourier transform it in θ to find the decay rates for individual modes. This scheme allows us to directly diagonalize the collision operator [Eq. (3)], finding the results shown in Fig. 1 (the relevant technical steps are described in Secs. C and D of the Supplemental Material).

The angular distribution of particles scattered after a test particle has been injected in the system at an energy near the

Fermi level, $f_i(\theta) = J_0\delta(\theta - \theta_i)$, is given by

$$f(\theta) = \oint \frac{d\theta'}{2\pi} \sigma(\theta - \theta') f_i(\theta') = \frac{J_0}{2\pi} \sigma(\theta - \theta_i), \qquad (5)$$

where $f_i(\theta)$ describes the injected beam and the scattering angle θ parametrizes the Fermi surface. Here, J_0 is a T-independent intensity of the injected beam and, for simplicity, we suppressed the width of the distribution in the radial direction. As discussed above, excitations with different lifetimes are represented as normal modes of the two-body collision operator linearized in the deviation of the distribution from the equilibrium state $I_{\mathrm{ee}}[f_m(\theta)] = -\gamma_m f_m(\theta)$, where γ_m are the decay rates (inverse lifetimes) for different excitations. Due to the cylindrical symmetry of the problem, the normal modes are the angular harmonics $f_m(\theta) = e^{im\theta}$ times some functions of the radial momentum variable [35]. Comparing to Eq. (5), we see that the quantities γ_m are related to the Fourier coefficients of the angle-resolved cross section,

$$\sigma(\theta) = \sum_m e^{im(\theta - \theta_i)}(\gamma_m - \gamma_0), \qquad (6)$$

where the term $-\gamma_0$ describes particle loss from the injected beam. We use the basis functions introduced above to compute $\sigma(\theta)$ and then use the relation in (6) to obtain the lifetimes of different modes.

The angular dependence, shown in Fig. 2, features sharp peaks centered at $\theta = 0$ and π, describing forward scattering and backscattering, respectively. The angular widths θ_T of the peaks scale as T at $T \ll T_F$. Notably, the backscattering peak is of a negative sign, representing backreflected holes. At $T \ll T_F$ the values $\sigma(\theta)$ at generic θ within the peak scale as T. Multiplying this by the peak width $\theta_T \sim T/T_F$ yields the net backscattering rate that scales as T^2/T_F, as expected from Fermi-liquid theory. This behavior is detailed in the insets in Fig. 2.

The decay rates γ_m for odd-m modes, obtained from the relation in (6), show a significant departure from a T^2 scaling. The even-m and odd-m rates, shown in Fig. 1, are similar at $T \sim T_F$ but have a very different behavior at $T < T_F$. This difference originates from the collinear character of scattering, manifesting in prominent peaks in $\sigma(\theta)$ in the forward and backward directions. The near-equal areas of these peaks and the negative sign of the backscattering peak suppress the odd-m Fourier harmonics of $\sigma(\theta)$, yielding small decay rates for these harmonics. The T dependence for the even-m harmonics agrees well with the T^2 law. The odd-m harmonics, to the contrary, have decay rates decreasing at low T much faster than T^2. For these harmonics, we observe scaling $\gamma_m \sim T^\alpha$ with α slightly below 4. This represents a "super-Fermi-liquid" suppression of the decay rates for odd-m harmonics.

It is interesting to mention that collinear scattering, manifesting in the sharp peaks in $\sigma(\theta)$ at $\theta = 0$ and π, is directly responsible for the log enhancement of the quasiparticle decay rates predicted from the self-energy analysis [28–34]. Indeed, the angle dependence near $\theta = 0$ and π is of the form $\sigma(\theta) \sim T^2/|\theta|$ and $T^2/|\theta - \pi|$, with the $1/|\theta|$ singularity rounded on the scale $\delta\theta \sim T/T_F$, as illustrated in Fig. 2. Integrating the angle-resolved cross section over θ yields a $\log(T_F/T)T^2$ total scattering cross section. This illustrates that the abnormally long-lived excitations with the decay rates that scale as T^4 rather than T^2, described in this Letter, and the seminal $\log(T_F/T)T^2$ decay rates [28–34], originate from the same phase-space constraints. Restricted phase space renders quasiparticle scattering a highly collinear process even when the microscopic interactions have a weak angular dependence.

Given these findings, there is a clear interest to find a simple explanation for the unique properties of long-lived excitations. To accomplish this, we have employed a clever method developed 50 years ago in Refs. [44–47] to tackle transport in 3D Fermi liquids. This approach involves linearizing the kinetic equation near thermal equilibrium at $T \ll T_F$ to transform it into a time-dependent Schrödinger equation with a reflectionless sech^2 potential, which can be solved exactly to predict the transport coefficients at $T \ll T_F$. We use this framework to explore the modification of this equation in the 2D case and find that, although the decay rates of most excitations follow the T^2 scaling, a unique set of nondecaying excitations emerge due to zero modes originating from the supersymmetric quantum mechanics, with one mode per each odd angular momentum.

In general, the six-dimensional integral operator I_{ee} in Eq. (3) has a complicated structure which in a general case is difficult to analyze. However, at $T \ll T_F$ the part of phase space in which transitions $12 \leftrightarrow 1'2'$ are not restricted by fermion exclusion is a thin annulus of radius p_F and a small thickness $\delta p \approx T/v \ll p_F$. One can therefore factorize the six-dimensional integration over $\boldsymbol{p}_2$, $\boldsymbol{p}_{1'}$, and $\boldsymbol{p}_{2'}$ in I_{ee} into a three-dimensional energy integral and a three-dimensional angular integral, and integrate over angles to obtain a closed-form equation for the radial dependence $\chi(x)$. This is done by noting that the delta functions $\delta_\epsilon \delta_p$ together with the conditions $|\boldsymbol{p}_1| \approx |\boldsymbol{p}_2| \approx |\boldsymbol{p}_{1'}| \approx |\boldsymbol{p}_{2'}| \approx p_F$ imply that the states 1, 2, 1', and 2' form two anticollinear pairs

$$\boldsymbol{p}_1 + \boldsymbol{p}_2 \approx 0, \quad \boldsymbol{p}_{1'} + \boldsymbol{p}_{2'} \approx 0. \quad (7)$$

The azimuthal angles therefore obey $\theta_1 \approx \theta_2 + \pi$, $\theta_{1'} \approx \theta_{2'} + \pi$. In a thin-shell approximation $\delta p \ll p_F$, this gives two delta functions $\delta(\theta_1 - \theta_2 - \pi)$, $\delta(\theta_{1'} - \theta_{2'} - \pi)$ that cancel two out of three angle integrals in I_{ee}, allowing us to rewrite the quantity $\eta_{1'} + \eta_{2'} - \eta_1 - \eta_2$ as

$$e^{im\theta_{1'}}[\chi(x_{1'}) + (-)^m \chi(x_{2'})] - e^{im\theta_1}[\chi(x_1) + (-)^m \chi(x_2)], \quad (8)$$

where χ is a shorthand for χ_m. Here, as above, the variables x_i denote particle energies scaled by temperature, $x = \beta(\epsilon_i - \mu)$. Subsequent steps differ for the even and odd m, because the contributions of $\chi(x_{1'})$ and $\chi(x_{2'})$ to I_{ee} cancel out for odd m and double for even m, since the quantity F in Eq. (3) is symmetric in $x_{1'}$ and $x_{2'}$. Focusing on the odd m and carrying out integration over the angle between $\boldsymbol{p}_1$ and $\boldsymbol{p}_{1'}$ yields

$$\tilde{F}\frac{d\chi(x_1)}{dt} = T^2 \int dx_2 dx_{1'} dx_{2'} F g \delta_x [\chi(x_1) - \chi(x_2)], \quad (9)$$

where $\tilde{F} = f_0(1 - f_0)$ and $\delta_x = \delta(x_1 + x_2 - x_{1'} - x_{2'})$. Here, T^2 originates from nondimensionalizing the energy variables x_i in the integral and the delta function, the dimensionless factor g is a result of angular integration, and the quantity F is defined above. Integration over energy variables $x_2, x_{1'}, x_{2'}$ extends throughout $-\infty < x_i < \infty$, as appropriate for $T \ll T_F$.

As a first step, we reverse the signs of the 1' and 2' variables: $x_{1'} \to -x_{1'}$, $x_{2'} \to -x_{2'}$. This transforms the integral equation in Eq. (9) to

$$\tilde{F}\frac{d\chi}{dt} = gT^2 \int dx_2 dx_{1'} dx_{2'} F_{121'2'} \delta_x^+ [\chi(x_1) - \chi(x_2)],$$
$$F_{121'2'} = f_0(x_1) f_0(x_2) f_0(x_{1'}) f_0(x_{2'}), \quad (10)$$

where $\delta_x^+ = \delta(x_1 + x_2 + x_{1'} + x_{2'})$. Next, we use the identities

$$\int dx_2 dx_{1'} dx_{2'} f_0(x_2) f_0(x_{1'}) f_0(x_{2'}) \delta_x^+ = \frac{1}{2}\frac{x_1^2 + \pi^2}{1 + e^{-x_1}}, \quad (11)$$

$$\int dx_{1'} dx_{2'} f_0(x_{1'}) f_0(x_{2'}) \delta_x^+ = -\frac{x_1 + x_2}{1 - e^{-x_1 - x_2}} \quad (12)$$

to carry out integration over $x_2, x_{1'}, x_{2'}$ in the first term and over $x_{1'}, x_{2'}$ in the second term. The equation can be further simplified using the substitution

$$\chi(x) = 2\cosh\left(\frac{x}{2}\right)\zeta(x) = (e^{x/2} + e^{-x/2})\zeta(x), \quad (13)$$

which gives an equation

$$\frac{d\zeta(x_1)}{dt} = -gT^2\left[\frac{x_1^2 + \pi^2}{2}\zeta(x_1) + \int dx_2 \frac{\bar{x}}{\sinh\bar{x}}\zeta(x_2)\right],$$

where $\bar{x} = (x_1 + x_2)/2$. Next, we reverse the sign of x_2, which brings the integral operator to the form of a convolution, separately for the even and odd functions $\zeta(x_2)$. For an even function $\zeta(-x_2) = \zeta(x_2)$ we have

$$\int dx_2 \frac{x_1 - x_2}{2\sinh\frac{x_1 - x_2}{2}}\zeta(x_2).$$

After Fourier transforming $\zeta(x) = \int dk e^{ikx}\psi(k)$ this gives a time-dependent Schrödinger equation with a sech^2 potential,

$$\partial_t \psi(k) = gT^2\left[\frac{1}{2}\psi''(k) - \left(\frac{\pi^2}{2} - \frac{\pi^2}{\cosh^2 \pi k}\right)\psi(k)\right]. \quad (14)$$

Unlike the 3D case, where after a similar transformation the T^2 scaling translates into a T^2 dependence of the decay rates, here the operator in (14) has a zero mode, $\psi_0(k) = \frac{1}{\cosh(\pi k)}$. Being a zero mode, this mode does not relax. The associated $\chi_0(x)$ can be found from the identity $\int d\xi \frac{e^{2\pi i \xi y}}{\cosh \pi \xi} = \frac{1}{\cosh \pi y}$, giving $\chi_0(x) = 1$. Returning to the energy variable, this yields the Fermi-surface-displacement mode $\delta f(x) = df_0/dx = f_0(1 - f_0)$, identical for all odd m.

In a similar manner, for odd functions $\zeta(-x_2) = -\zeta(x_2)$, upon changing x_2 to $-x_2$, a minus sign appears in front of the integral operator:

$$-\int dx_2 \frac{x_1 - x_2}{2 \sinh \frac{x_1 - x_2}{2}} \zeta(x_2).$$

Carrying out the Fourier transform $\zeta(x) = \int dk e^{ikx} \psi(k)$ gives a time-dependent Schrödinger equation for a sech^2 potential of an opposite sign,

$$\partial_t \psi(k) = gT^2 \left[\frac{1}{2} \psi''(k) - \left(\frac{\pi^2}{2} + \frac{\pi^2}{\cosh^2 \pi k} \right) \psi(k) \right]. \quad (15)$$

In this case, physical solutions correspond to the eigenfunctions that are odd in k. For a repulsive sech^2 potential these functions are in the continuum spectrum and asymptotically have the form of plane waves. As a result, the behavior of the eigenfunctions that are odd in x is quite different from that of the even-x eigenfunctions discussed above.

For even m, analysis proceeds in an overall similar manner, yielding analytic expressions for the eigenstates and associated eigenvalues. However, the 1D Schrödinger operators obtained for even m feature no zero modes. As a result, the analysis yields a normal T^2 scaling of the decay rates. This is so because for even m the terms $\chi(x_1')$ and $\chi(x_2')$ in (8) are of equal signs and do not cancel out. As a result, the even-m and odd-m harmonics show a very different behavior: The odd-m rates vanish in the zero-thickness approximation for the active shell at the Fermi surface, whereas the even-m rates remain finite in this limit, scaling as T^2.

We would like to note that, while the 1D quantum mechanics approach is fully adequate for tackling even-m excitations, the problem of odd-m excitations remains open and requires further investigation. Infinite lifetimes found for odd-m modes and interpreted in terms of zero modes, merely indicate that the decay rates for these modes vanish at order T^2. However, the supersymmetry that protects zero eigenvalues is a property that only appears in the limit of zero thickness of the thermally broadened Fermi surface. Therefore, it is unlikely that this property holds outside of this limit, and we expect the lifetimes of odd-m modes to be finite. Our numerical results indicate that the decay rates for these modes scale as T^α, with $\alpha > 2$. However, determining the values of α analytically may require a framework that extends beyond the approximations considered in our 1D quantum mechanics approach.

Further research is needed to understand the behavior of odd-m excitations, and we hope that our work will inspire future forays into this intriguing problem. The relation with the 1D supersymmetric quantum mechanics can be employed, in principle, to study a variety of other problems of interest, e.g., the thermal transport effects such as thermal conduction, the Joule-Thomson effect, and convective thermal drag. A comprehensive understanding of these transport effects would require deriving transport equations for these quantities supplied with suitable boundary conditions and connecting them to observables. This is an interesting topic for future work.

In summary, the kinematic restrictions of the phase space for quasiparticle scattering at the Fermi surface lead to highly collinear dynamics, even if the microscopic interactions have weak angular dependence. This gives rise to several notable effects, such as the emergence of abnormally long-lived excitations and strong backscattering features in the angular distribution for two-body collisions. The resulting unusual kinetics is especially relevant for 2D systems that are currently being investigated for electron hydrodynamics and related collective phenomena. Long-lived degrees of freedom can amplify the response to weak perturbations, giving rise to long-lasting collective memory effects and new hydrodynamic modes. This is illustrated by a family of viscous modes with non-Newtonian viscosity and transport phenomena due to these modes described in Ref. [27]. This area of transport theory is rapidly evolving, and a robust understanding of the fundamental physics behind collinear collisions is crucial to grasp the electron behavior in various transport phenomena.

---

[1] M. Müller, J. Schmalian, and L. Fritz, Graphene: A Nearly Perfect Fluid, Phys. Rev. Lett. **103**, 025301 (2009).

[2] A. Tomadin, G. Vignale, and M. Polini, A Corbino Disk Viscometer for 2D Quantum Electron Liquids, Phys. Rev. Lett. **113**, 235901 (2014).

[3] A. Principi, G. Vignale, M. Carrega, and M. Polini, Bulk and shear viscosities of the two-dimensional electron liquid in a doped graphene sheet, Phys. Rev. B **93**, 125410 (2016).

[4] T. Scaffidi, N. Nandi, B. Schmidt, A. P. Mackenzie, and J. E. Moore, Hydrodynamic Electron Flow and Hall Viscosity, Phys. Rev. Lett. **118**, 226601 (2017).

[5] A. Lucas and K. C. Fong, Hydrodynamics of electrons in graphene, J. Phys.: Condens. Matter **30**, 053001 (2018).

[6] K. A. Guerrero-Becerra, F. M. D. Pellegrino, and M. Polini, Magnetic hallmarks of viscous electron flow in graphene, Phys. Rev. B **99**, 041407(R) (2019).

[7] B. N. Narozhny and M. Schütt, Magnetohydrodynamics in graphene: Shear and Hall viscosities, Phys. Rev. B **100**, 035125 (2019).

[8] P. S. Alekseev and A. P. Dmitriev, Viscosity of two-dimensional electrons, Phys. Rev. B **102**, 241409(R) (2020).

[9] R. Toshio, K. Takasan, and N. Kawakami, Anomalous hydrodynamic transport in interacting noncen-

trosymmetric metals, Phys. Rev. Res. **2**, 032021(R) (2020).

[10] B. N. Narozhny, I. V. Gornyi, and M. Titov, Hydrodynamic collective modes in graphene, Phys. Rev. B **103**, 115402 (2021).

[11] E. H. Hasdeo, J. Ekström, E. G. Idrisov, and T. L. Schmidt, Electron hydrodynamics of two-dimensional anomalous Hall materials, Phys. Rev. B **103**, 125106 (2021).

[12] M. Qi and A. Lucas, Distinguishing viscous, ballistic, and diffusive current flows in anisotropic metals, Phys. Rev. B **104**, 195106 (2021).

[13] C. Q. Cook and A. Lucas, Viscometry of Electron Fluids from Symmetry, Phys. Rev. Lett. **127**, 176603 (2021).

[14] D. Valentinis, J. Zaanen, and D. van der Marel, Propagation of shear stress in strongly interacting metallic Fermi liquids enhances transmission of terahertz radiation, Sci. Rep. **11**, 7105 (2021).

[15] D. Valentinis, Optical signatures of shear collective modes in strongly interacting Fermi liquids, Phys. Rev. Res. **3**, 023076 (2021).

[16] J. Hofmann and S. Das Sarma, Collective modes in interacting two-dimensional tomographic Fermi liquids, Phys. Rev. B **106**, 205412 (2022).

[17] H. Guo, E. Ilseven, G. Falkovich, and L. Levitov, Higher-than-ballistic conduction of viscous electron flows, Proc. Natl. Acad. Sci. USA **114**, 3068 (2017).

[18] A. V. Shytov, J. F. Kong, G. Falkovich, and L. S. Levitov, Particle Collisions and Negative Nonlocal Response of Ballistic Electrons, Phys. Rev. Lett. **121**, 176805 (2018).

[19] K. G. Nazaryan and L. S. Levitov, Robustness of vorticity in electron fluids, arXiv:2111.09878.

[20] R. N. Gurzhi, A. N. Kalinenko, and A. I. Kopeliovich, Electron-Electron Collisions and a New Hydrodynamic Effect in Two-Dimensional Electron Gas, Phys. Rev. Lett. **74**, 3872 (1995).

[21] H. Buhmann and L. W. Molenkamp, 1D diffusion: A novel transport regime in narrow 2DEG channels, Physica E **12**, 715 (2002).

[22] P. J. Ledwith, H. Guo, and L. Levitov, Angular superdiffusion and directional memory in two-dimensional electron fluids, arXiv:1708.01915.

[23] P. Ledwith, H. Guo, A. Shytov, and L. Levitov, Tomographic Dynamics and Scale-Dependent Viscosity in 2D Electron Systems, Phys. Rev. Lett. **123**, 116601 (2019).

[24] P. J. Ledwith, H. Guo, and L. Levitov, The hierarchy of excitation lifetimes in two-dimensional Fermi gases, Ann. Phys. **411**, 167913 (2019).

[25] T. Giamarchi, *Quantum Physics in One Dimension* (Clarendon Press, Oxford, UK, 2004).

[26] G. Giuliani and G. Vignale, *Quantum Theory of the Electron Liquid* (Cambridge University Press, Cambridge, UK, 2012).

[27] S. Kryhin and L. Levitov, Non-Newtonian hydrodynamic modes in two-dimensional electron fluids, arXiv:2305.02883.

[28] C. Hodges, H. Smith, and J. W. Wilkins, Effect of Fermi surface geometry on electron-electron scattering, Phys. Rev. B **4**, 302 (1971).

[29] A. V. Chaplik, Energy spectrum and electron scattering processes in inversion layers, Zh. Eksp. Teor. Fiz. **60**, 1845 (1971) [Sov. Phys. JETP **33**, 997 (1971)].

[30] P. Bloom, Two-dimensional Fermi gas, Phys. Rev. B **12**, 125 (1975).

[31] G. F. Giuliani and J. J. Quinn, Lifetime of a quasiparticle in a two-dimensional electron gas, Phys. Rev. B **26**, 4421 (1982).

[32] L. Zheng and S. Das Sarma, Coulomb scattering lifetime of a two-dimensional electron gas, Phys. Rev. B **53**, 9964 (1996).

[33] D. Menashe and B. Laikhtman, Quasiparticle lifetime in a two-dimensional electron system in the limit of low temperature and excitation energy, Phys. Rev. B **54**, 11561 (1996).

[34] A. V. Chubukov and D. L. Maslov, Nonanalytic corrections to the Fermi-liquid behavior, Phys. Rev. B **68**, 155113 (2003).

[35] See Supplemental Material at http://link.aps.org/supplemental/10.1103/PhysRevB.107.L201404 for a detailed description of the numerical method used for determining the collision operator eigenfunctions and eigenvalues.

[36] J. González, F. Guinea, and M. A. H. Vozmediano, Unconventional Quasiparticle Lifetime in Graphite, Phys. Rev. Lett. **77**, 3589 (1996).

[37] D. Brida, A. Tomadin, C. Manzoni, Y. J. Kim, A. Lombardo, S. Milana, R. R. Nair, K. S. Novoselov, A. C. Ferrari, G. Cerullo, and M. Polini, Ultrafast collinear scattering and carrier multiplication in graphene, Nat. Commun. **4**, 1987 (2013).

[38] J. C. W. Song, K. J. Tielrooij, F. H. L. Koppens, and L. Levitov, Photoexcited carrier dynamics and impact-excitation cascade in graphene, Phys. Rev. B **87**, 155429 (2013).

[39] Q. Li and S. Das Sarma, Finite temperature inelastic mean free path and quasiparticle lifetime in graphene, Phys. Rev. B **87**, 085406 (2013).

[40] U. Briskot, I. A. Dmitriev, and A. D. Mirlin, Relaxation of optically excited carriers in graphene: Anomalous diffusion and Lévy flights, Phys. Rev. B **89**, 075414 (2014).

[41] M. Trushin, Collinear scattering of photoexcited carriers in graphene, Phys. Rev. B **94**, 205306 (2016).

[42] C. Lewandowski and L. Levitov, Photoexcitation Cascade and Quantum-Relativistic Jets in Graphene, Phys. Rev. Lett. **120**, 076601 (2018).

[43] E. I. Kiselev and J. Schmalian, Lévy Flights and Hydrodynamic Superdiffusion on the Dirac Cone of Graphene, Phys. Rev. Lett. **123**, 195302 (2019).

[44] G. A. Brooker and J. Sykes, Transport Properties of a Fermi Liquid, Phys. Rev. Lett. **21**, 279 (1968).

[45] H. Højgård Jensen, H. Smith, and J. Wilkins, Exact transport coefficients for a Fermi liquid, Phys. Lett. A **27**, 532 (1968).

[46] J. Sykes and G. A. Brooker, The transport coefficients of a Fermi liquid, Ann. Phys. (NY) **56**, 1 (1970).

[47] G. Baym and C. Pethick, *Landau Fermi-Liquid Theory: Concepts and Applications* (Wiley, New York, 1991).